Cancer Research

Expansion of Tumor-Infiltrating CD8$^+$ T cells Expressing PD-1 Improves the Efficacy of Adoptive T-cell Therapy

Sarita M. Fernandez-Poma[1,2], Diego Salas-Benito[2,3], Teresa Lozano[1,2], Noelia Casares[1,2], Jose-Ignacio Riezu-Boj[2,4], Uxua Mancheño[1,2], Edurne Elizalde[1,2], Diego Alignani[2,5], Natalia Zubeldia[1,2], Itziar Otano[1,2], Enrique Conde[1,2], Pablo Sarobe[1,2], Juan Jose Lasarte[1,2], and Sandra Hervas-Stubbs[1,2]

Abstract

Recent studies have found that tumor-infiltrating lymphocytes (TIL) expressing PD-1 can recognize autologous tumor cells, suggesting that cells derived from PD-1$^+$ TILs can be used in adoptive T-cell therapy (ACT). However, no study thus far has evaluated the antitumor activity of PD-1–selected TILs *in vivo*. In two mouse models of solid tumors, we show that PD-1 allows identification and isolation of tumor-specific TILs without previous knowledge of their antigen specificities. Importantly, despite the high proportion of tumor-reactive T cells present in bulk CD8 TILs before expansion, only T-cell products derived from sorted PD-1$^+$, but not from PD-1$^-$ or bulk CD8 TILs, specifically recognized tumor cells. The fold expansion of PD-1$^+$ CD8 TILs was 10 times lower than that of PD-1$^-$ cells, suggesting that outgrowth of PD-1$^-$ cells was the limiting factor in the tumor specificity of cells derived from bulk CD8 TILs. The highly differentiated state of PD-1$^+$ cells was likely the main cause hampering *ex vivo* expansion of this subset. Moreover, PD-1 precisely identified marrow-infiltrating, myeloma-specific T cells in a mouse model of multiple myeloma. *In vivo*, only cells expanded from PD-1$^+$ CD8 TILs contained tumor progression, and their efficacy was enhanced by PDL-1 blockade. Overall, our data provide a rationale for the use of PD-1–selected TILs in ACT. *Cancer Res; 77(13); 3672–84. ©2017 AACR.*

Introduction

Cancer immunotherapy based on ACT using autologous tumor-infiltrating lymphocytes (TIL) has been shown to mediate durable complete responses in refractory metastatic melanoma (1, 2). TILs are naturally occurring T cells able to recognize tumor-associated antigens (Ag), including neo-Ags (3). This can explain the highly specific antitumor responses and the low toxicity of TILs in comparison with genetically modified T cells expressing transgenic T-cell receptors (TCR) or chimeric antigen receptors (4). Moreover, TILs are heterogeneous in their specificity (3, 5), an important advantage for impeding tumor immunologic escape, and ACT using TILs is not limited to the previous knowledge of specific tumor Ags or to the patient's HLA.

One of the major constraints of TIL therapy is the complex TIL-manufacturing process. The procedure starts with multiwell cultures of tumor fragments or single-cell suspensions obtained from disaggregated tumors, in the presence of high dose of IL2 (6). After this initial culture lasting 3–5 weeks, the tumor reactivity of different wells is tested by coculturing TIL samples with autologous tumor cells (6). The reactive sublines are then chosen for large-scale secondary polyclonal expansion during two additional weeks to generate the final product (6). This method is known as the "selected TIL" approach and has been the basis of most of the TIL clinical trials performed in melanoma patients at the National Cancer Institute (7). To avoid the need to establish autologous tumor cell lines that are not available in many cases, more recent protocols circumvent measuring tumor reactivity and use bulk "unselected TILs" expanded after the initial outgrowth for further amplification (8). This approach has reported objective responses, albeit at a level significantly lower than those reported using "selected TILs" (8–10).

A critical parameter in TIL therapy is ensuring that the starting TIL culture has significant autologous tumor reactivity and maintained this reactivity after *ex vivo* expansion. During the expansion process there is an interclonal competition with different T-cell clones increasing or decreasing in frequency. Given this interclonal competition, the more tumor-specific clones in the starting culture, the greater the chance of maintaining tumor-specific clones at an appreciable frequency in the final product. Therefore, enrichment for tumor-specific T-cell subsets immediately before the expansion phase might eventually enhance the tumor reactivity of the final cellular product and simplify the TIL production process.

[1]Program of Immunology and Immunotherapy, Center for Applied Medical Research (CIMA), University of Navarra, Navarra, Spain. [2]Instituto de Investigación Sanitaria de Navarra (IdISNA), Navarra, Spain. [3]Oncology Department, University Clinic, University of Navarra, Navarra, Spain. [4]Centre for Nutrition Research, University of Navarra, Navarra, Spain. [5]Cytometry Unit, CIMA, University of Navarra, Navarra, Spain.

Note: Supplementary data for this article are available at Cancer Research Online (http://cancerres.aacrjournals.org/).

J.J. Lasarte and S. Hervas-Stubbs contributed equally to this article.

Corresponding Author: Sandra Hervas-Stubbs, Center for Applied Medical Research (CIMA), University of Navarra, Avenida Pio XII 55, Pamplona, Navarra 31008, Spain. Phone: 34-948-194-700; Fax: 34-948-194-717; E-mail: mshervas@unav.es

doi: 10.1158/0008-5472.CAN-17-0236

An important issue is how to distinguish tumor-specific T cells from other unrelated T cells present in the tumor infiltrate without knowing the specific Ag targeted. Tumor-reactive T cells express several activation-associated molecules, such as CD137, as a product of specific recognition of tumor cells (11–13). Similarly, negative checkpoint molecules, such as PD-1, are induced upon T-cell activation (14–16). Recent studies in melanoma and ovarian cancer patients have found that $CD8^+PD\text{-}1^+$ and $CD8^+CD137^+$ T cells can be specifically isolated from tumor infiltrates and that most antitumor reactivity is harbored in these isolated subsets (13, 17, 18). This discovery offers the opportunity to selectively isolate these T-cell subsets from tumors and expand them directly for infusion. Some controversy has arisen regarding which molecule on TILs, PD-1 or CD137, are better when selecting the tumor-specific populations (13, 18). As a large majority of CD8 T cells isolated from melanoma and other solid tumors express PD-1, whereas CD137 expression is much lower and tightly confined to the $PD\text{-}1^+$ subset (13, 18), PD-1 has received more attention for TIL selection.

One potential concern with isolating T cells expressing $PD\text{-}1^+$ for therapy is that these cells may be exhausted or functionally impaired (15). These issues, together with the adaptive resistance response of tumors through the expression of PD-1 ligands, may undermine the therapeutic efficacy of cells expanded from the $PD\text{-}1^+$ TIL subset. Indeed, to date, no study has addressed the *in vivo* antitumor activity of PD-1–selected TILs. Using mouse models of solid and hematologic tumors, we have investigated the therapeutic potential of PD-1–selected CD8 TILs and have compared this with that of total and $PD\text{-}1^-$ CD8 TILs. In addition, we have analyzed the fold expansion capacity, the tumor reactivity, and the TCR repertoire of all these TIL subsets after *ex vivo* expansion.

Materials and Methods

Mice and tumor cell lines

C57BL/6 (BL6) and C57BL/KaLwRij (C57BL/K) mice were obtained from Harlan Laboratories. CD45.1 mice (B6.SJL-Ptprca-Pep3b/BoyJ mice) were from Jackson Laboratory. All animal handling and tumor experiments were approved by our institutional ethics committee (012-15) in accordance with Spanish regulations. The mouse colon adenocarcinoma MC38 cell line (19) and the mouse melanoma B16F10 cells expressing OVA (B16OVA; ref. 20) were obtained in 2013 from Dr. Melero (Center for Applied Medical Research, Spain), who verified both cell lines by Idexx Radil in 2012. ID8 cells (mouse epithelial ovarian cancer cells) were obtained (April 30, 2015) from Dr. Roby (Kansas University Medical Center, Kansas City, KS; ref. 21) and authenticated by STR-DNA profiling (November 5, 2015). The murine myeloma 5TGM1 cell line and 5TGM1 cells expressing GFP (5TGM1-GFP; ref. 22) were obtained (June 17, 2016) from Dr. Oyajobi (University of Texas Health Science Center, Houston, TX). These cells were not authenticated; however, confirmation of secretion of the specific IgG2bκ paraprotein and tumor formation in the C57BL/K syngeneic mouse strain provided evidence of correct cell identity. EL4 cells were acquired (March 6, 2013) from ATCC (ATCC-TIB-39). Authenticated batches were cryopreserved and the master bank (N_2L). One vial from the master bank was used to produce the working bank. Cells with 1–2 passages from the working bank were used in the experiments. All these cells lines were certified as being Mycoplasma-free by using the MycoAlert Mycoplasma Detection Kit (Lonza).

Tumor inoculation and processing

B16OVA cells (5×10^5) were injected subcutaneously into the flanks of BL6 mice. Advanced liver metastasis from colon adenocarcinoma was mimicked by injection of MC38 cells (5×10^5) into the main liver lobe. Fifteen days later, excised tumors were digested with 400 U/mL collagenase D and 50 μg/mL DNase-I (Roche). A total of 5×10^6 5TGM1-GFP cells were injected intravenously in C57BL/K mice. Multiple myeloma development was confirmed by detection of seric IgG2bκ paraprotein by ELISA (23).

Flow cytometry

Cells were incubated with Zombie NIR Fixable dye (Biolegend). Subsequently, they were stained with phycoerythrin-labeled H-$2K^b/OVA_{257\text{-}264}$– or H-$2K^b$/M8 (MuLV $p15E_{604\text{-}611}$)-tetramers (MBL) and then with fluorochrome-conjugated mAbs against CD8, CD4 (RM4-5), CD3ε (145-2C11), NK1.1 (PK136), PD-1 (HA2-7B1), LAG-3 (C9B7W), 2B4 [m2B4(B6)458.1], GITR (DTA-1), CD137 (17b5-1H1), ICOS (398.4A), CD44 (IM7), CCR7 (4B12), CD62L (MEL-14), and KLRG1 (2F1) in the presence of purified anti-CD16/32 mAb. For intracellular staining, cells were fixed and permeabilized with the Foxp3 Staining kit buffer (eBiosciences) and then stained with anti-CTLA-4 (9H10), -CD40L (MR1), -granzyme B (GB11), and -FoxP3 (FJK-16s) mAbs. Samples were acquired on a FACSCanto-II cytometer (BD Biosciences). The stopping gate was "total CD8" ($ZombieNIR^-CD3^+NK1.1^-CD8^+$ cells). We acquired a minimum of 2,000 "total CD8" events. Data were analyzed using FlowJo software (TreeStar).

Sorting and expansion of CD8 TIL subsets

Cells from digested solid tumors or splenocytes and bone marrow cells from multiple myeloma–bearing mice were cultured overnight [RPMI-1640-Glutamax (Gibco) with 10% heat-inactivated FBS (Sigma-Aldrich), 100 U/mL penicillin, and 100 mg/mL streptomycin (Invitrogen)]. Then, cells were stained with mAbs against CD8 (53-6.7) and PD-1 [HA2-7B1 (Miltenyi Biotec) and 29F.1A12 (Biolegend)]. In some experiments, anti-CD137 (17b5-1H1) and -CD62L (MEL-14) mAbs were also used to sort cells. Sorting of $CD8^+$ subsets was performed in a FACSAria sorter. Aggregates and dead cells ($7AAD^+$) were excluded. FACS-sorted CD8 T cells were expanded using a modified rapid expansion protocol that uses irradiated (4,000 rads) allosensitized allogeneic lymphocytes (ASAL) and dendritic cells (DC; ref. 24). TILs, ASALs, and DCs were cultured at a 1:4:1 ratio in the presence of soluble anti-CD3 mAb (145-2c11, 50 ng/mL) and human IL2 (1,500 IU/mL; Proleukin; ref. 24). Cells were split to maintain a concentration of $0.5–2 \times 10^6$ cells/mL. In some experiments, cells were cultured in the presence of anti-PD-1–blocking mAbs (clone RMP1-14) or rat IgG2a (10 μg/mL). The absolute number of TILs throughout the culture process was assessed by flow cytometry using anti-CD3, -CD8 and -CD45.1 mAbs, 7AAD, and Perfect-Count Microspheres (Cytognos). TILs were identified as $CD3^+CD8^+CD45.1^-7AAD^-$ cells. Absolute counts of TILs were calculated by determining the beads:TIL ratio and then multiplying this ratio by the number of beads in the tube.

Generation of ASALs and DCs

ASALs were generated over 7 days by coculturing splenocytes from a donor mouse (CD45.1) with irradiated (4,000 rads) splenocytes from a second donor mouse (BALBc) at a 1:1 ratio

in the presence of IL2 (100 IU/mL; ref. 24). Bone marrow cells from BALB/c mice were differentiated over 6 days into DCs with GM-CSF (20 ng/mL) and then maturated for 24 hours with LPS (1 μg/mL, Invivogen).

Tumor reactivity assays

Freshly isolated TILs or cells expanded for 9–10 days and rested overnight in medium without IL2 (effector cells) were tested for their tumor specificity by coculture with the related tumor cell line or with unrelated tumor cells (target cells) and measuring the IFNγ production (by ELISA or ELISPOT) or CD137 upregulation. For detection of IFNγ by ELISA, effector cells (10^5) were cultured (24 hours) either alone or with target cells (E:T ratio = 1:1) and the amount of secreted IFNγ was measured using the BD OptEIA mouse IFNγ ELISA Set (BD Biosciences). For IFNγ-ELISPOT, effector cells (5×10^4 cells/well) were cultured either alone or with target cells (E:T=10:1) in ELIIP plates (Millipore) coated with purified anti-IFNγ mAb (AN18; Mabtech). Twenty hours later, cells were harvested for detection of CD137 by flow cytometry and the plate was developed using biotinylated anti-IFNγ mAb (R4-6A2), streptavidin-ALP, and BCIP/NBT substrate (Mabtech). Plates were analyzed using a CTL-ImmunoSpot S6 Micro-Analyzer-Cellular Technology.

ACT experiments

In micrometastases models, B16OVA or MC38 tumor cells (5×10^5) were injected intravenously into 8-week-old BL6 mice and 3 days later therapy was instituted with (2×10^6) or without TILs in combination with systemic administration of IL2 (two daily injections of 2×10^4 IU of IL2 every 12 hours during 4 days). In the model of large established tumors, BL6 mice were injected subcutaneously with 5×10^5 B16OVA tumor cells. Mice bearing 6-day or 10-day B16OVA tumors received total body irradiation (TBI; 500 rads) and therapy was instituted with (10^7) or without TILs. In addition, all mice received systemically IL2 as before. TILs from day 9 of culture were used for ACT. In some experiments, mice received a single injection of rat IgG or anti-PDL-1 mAbs (10F.9G2; 100 μg) the day after ACT. As a control, groups of mice received anti-PD-L1, either with or without previous TBI, and IL2.

Statistical analysis

GraphPad software was used to analyze differences between groups by statistic tests as specified in the figure legends. All tests were two-tailed and conducted at 95% of confidence.

Results

MHC/peptide tetramer reactivity and PD-1 expression merge in TILs

To identify markers that allow isolation of tumor-reactive TILs, we first characterized well-known tumor-specific T cells from the B16OVA model with the aid of two H-2K^b-tetramers bearing immunodominant T-cell epitopes from this tumor (the OVA- and the M8-tetramer; ref. 25). First, we assessed the relative expression of several coinhibitory and costimulatory molecules on total CD8$^+$, tetramer$^+$CD8$^+$, CD4$^+$FoxP3$^-$ (Th), and CD4$^+$FoxP3$^+$ (Treg) TILs from 15-day tumor-bearing mice (Fig. 1A-C). Almost all OVA- and M8-specific T cells (>97%) expressed PD-1 and a high proportion expressed LAG-3 (>85%) and 2B4 (70%), compared with CD4$^+$ TILs (Fig. 1B). Essentially all Tregs and 42% of Th cells expressed high levels of CTLA-4, whereas 35%–46% of tetramer$^+$ cells showed a smeared pattern of CTLA-4 expression (Fig. 1B). Approximately 87% and 55% of tetramer$^+$ cells expressed GITR and CD137, respectively (Fig. 1C). These two molecules were also detected in the CD4$^+$ compartments, especially GITR, which was expressed by >90% and 60% of Treg and Th cells, respectively. ICOS expression was largely circumscribed to Tregs and a small subset of Th cells, whereas CD40L was detected only faintly in CD8$^+$ and CD4$^+$ TILs. Characterization of intrahepatic MC38 TILs specific for the M8 epitope (also expressed in the MC38 cell line) from 15-day tumor-bearing mice mirrored findings in the B16OVA model (Supplementary Fig. S1A and S1B). Supplementary Figure S1C summarizes the expression level of all these coinhibitory and costimulatory molecules on tetramer$^+$ CD8 TILs and other TIL subsets. At day 15 after tumor injection, PD-1 and LAG-3 more distinctly demarcated tetramer$^+$ T cells from the rest of TILs.

To understand how natural tumor-specific TILs acquired the expression of coinhibitory and costimulatory molecules over the course of tumor progression, we assessed the phenotype of tetramer$^+$ CD8 TILs from B16OVA tumor-bearing mice at different time points after tumor injection. M8-specific CD8 TILs were detected early (day 6) in tumor infiltrate, and during tumor development their frequency was always higher than that of OVA-specific TILs, becoming 60%–80% of total CD8 TIL population in large tumors (day 24; Supplementary Fig. S2A and S2B). Because of the low number of OVA-tetramer$^+$ TILs at days 6 and 12, we focused on the phenotype of M8-tetramer$^+$ cells. By day 6, PD-1, LAG-3, and ICOS were the receptors most overexpressed in M8-specific TILs (Supplementary Fig. S2C and S2D). The expression of PD-1, LAG-3, 2B4, CTLA-4, and GITR increased over time, with 2B4 peaking at day 18. Interestingly, CD137 reached its peak early on day 12, whereas ICOS steadily fell along tumor progression. Levels of expression of all these markers were similar in tetramer$^+$ cells and PD-1$^+$ CD8 TILs (Supplementary Fig. S2C). From day 18, the expression levels of all these activation-dependent molecules were similar in bulk and PD-1$^+$ CD8 TILs, most likely due to the progressive increase of PD-1$^+$ cells within CD8 TILs (Supplementary Fig. S2C)

Notably, over the course of tumor progression, LAG-3, 2B4, CTLA-4, GITR, CD137, and ICOS were mostly expressed on PD-1$^+$ cells (Fig. 1D; Supplementary Fig. S2D). PD-1$^+$ CD8 TILs also expressed high levels of granzyme B and CD44 and low levels of CD62L, CCR7, and KLRG1 exhibiting a T effector memory (TEM) phenotype (Fig. 1E). Overall, the unique coexpression profile of PD-1 with the other activation-dependent molecules and the fact that >90% of tetramer$^+$ cells expressed PD-1 in well-established tumors, prompted us to study PD-1$^+$ CD8 TILs in greater detail.

PD-1 in the fresh tumor identifies the full repertoire of tumor-reactive CD8 TILs without the need to know epitope specificities

To determine whether a proportion of tumor-reactive CD8 TILs could be missed in the PD-1$^-$ T-cell compartment, we sorted CD8 TILs into PD-1$^-$ and PD-1$^+$ (Fig. 2A) and assessed the tumor reactivity of freshly isolated TILs by IFNγ-ELISPOT using the related tumor cell line (B16OVA) as target cells. ID8 cells were used as unrelated tumor cells to assess nonspecific reactions. As depicted in Fig. 2B, only PD-1$^+$ CD8 TILs were able to specifically recognize B16OVA cells. These data indicate that expression of PD-1 in the fresh tumor can be used to identify tumor-reactive CD8 TILs without previous knowledge of their Ag specificities.

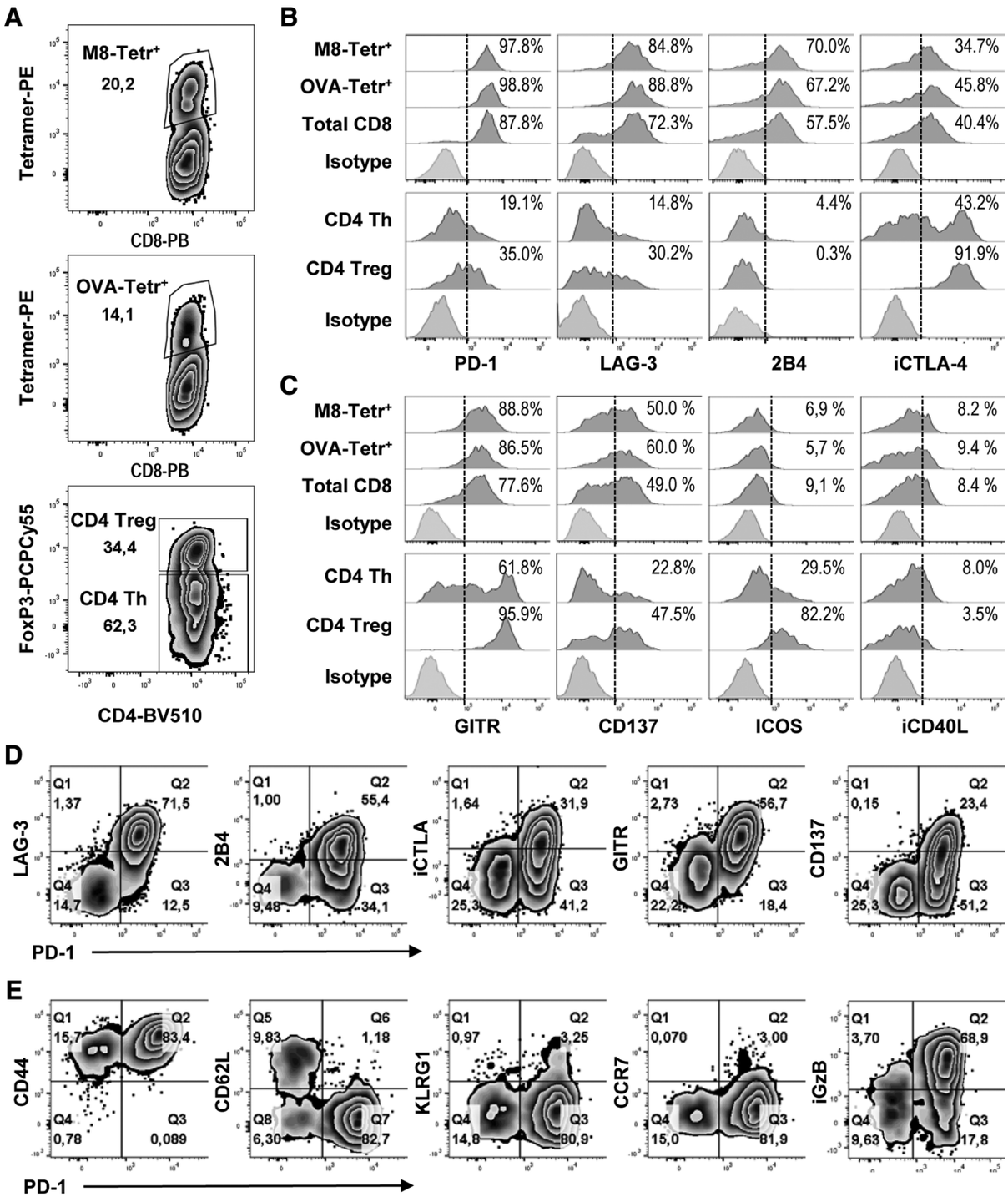

Figure 1.

Multiparametric flow cytometric analysis of tumor-infiltrating T lymphocyte subsets from freshly excised B16OVA tumors. B16OVA cells were subcutaneously injected in BL6 mice and 15 days later the cellular suspension obtained from tumor digestion was analyzed by flow cytometry. **A,** TIL subsets analyzed by multiparametric flow cytometry. **B** and **C,** Relative expression of coinhibitory (**B**) and costimulatory (**C**) molecules. Histograms display surface expression of PD-1, LAG-3, 2B4, CD137, GITR, and ICOS, and intracellular expression of CTLA-4 and CD40L (iCTLA-4 and iCD40L, respectively) by M8-tetramer$^+$, OVA-tetramer$^+$, total CD8, CD4$^+$FoxP3$^-$ (Th), and CD4$^+$FoxP3$^+$ (Treg). **D** and **E,** Dot plots showing relative expression of surface PD-1 against surface LAG-3, 2B4, GITR, CD137, CD44, CD62L, and KLRG1 and against intracellular CTLA-4 (iCTLA4) and granzyme B (iGzB) by total CD8 T cells from B16OVA tumors. **B–E,** Appropriate isotype controls were used to verify the specificity of the staining. One mouse representative of 14 mice tested in three independent experiments (n = 4–6 mice/experiment).

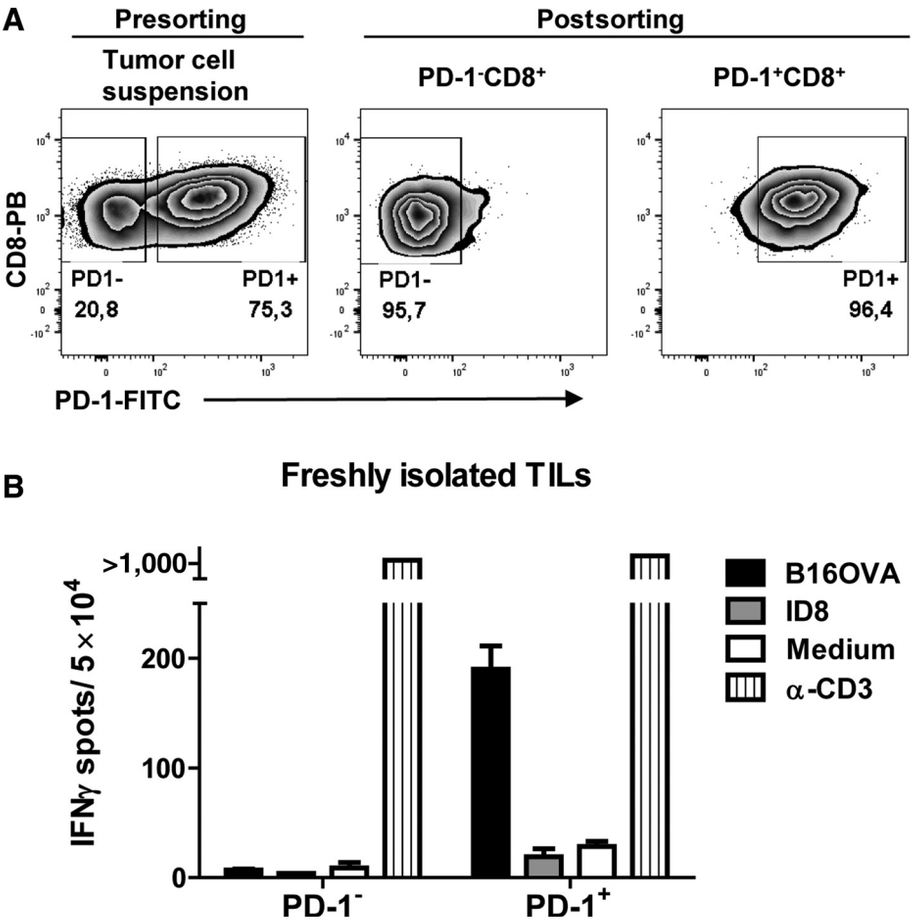

Figure 2.
PD-1 in the fresh tumor identifies the full repertoire of tumor-reactive CD8 TILs without the need to know Ag specificities. **A** and **B,** Cellular suspension obtained from 15-day sc B16OVA tumors was sorted into PD-1$^-$ and PD-1$^+$ CD8 T cells. **A,** Isolated CD8 TIL subsets. Panel showing cells before sorting was gated on live CD8 T cells. Panels showing CD8 TIL subsets after sorting was gated on total live cells. **B,** Freshly isolated T cells were cultured with B16OVA and unrelated (ID8) tumor cells for 20 hours. Tumor-specific reactivity was determined by IFNγ-ELISPOT assay. As a control, T cells were cultured in wells coated with anti-CD3 (145-2C11, 0.1 μg/mL) and anti-IFNγ mAb or with culture medium alone. Greater than 40 spots and greater than twice the background was considered positive T-cell reactivity. Mean ± SD of three culture replicates. One experiment representative of two experiments is shown.

Some controversy has arisen regarding which molecule on CD8 TILs, PD-1 or CD137, better identifies the tumor-specific T-cell populations (13, 18). To contribute to clarify this issue, we separated CD8 TILs from B16OVA tumors into PD-1$^-$/CD137$^-$, PD-1$^+$/CD137$^+$, and PD-1$^+$/CD137$^-$, but not PD-1$^-$/CD137$^+$, due to its low frequency (Fig. 1D), as has also been described in patients with melanoma (18). Both PD-1$^+$/CD137$^+$ and PD-1$^+$/CD137$^-$ subsets contained comparable numbers of tumor-reactive T cells (Supplementary Fig. S3A). Curiously, PD-1$^+$/CD137$^+$ cells spontaneously produced IFNγ. Similar data were obtained in the MC38 model (Supplementary Fig. S3D). These data indicate that expression of PD-1 and CD137 in the fresh tumor can be used to identify tumor-specific T cells. However, as a significant fraction of tumor-reactive T cells was found in the PD-1$^+$/CD137$^-$ compartment, PD-1, rather than CD137, more precisely encompasses the repertoire of tumor-specific T cells.

PD-1$^+$ CD8 TILs expand *ex vivo* although less efficiently than their PD-1$^-$ counterparts

To assess the expansion capacity of PD-1$^+$ TILs, we sorted TILs from B16OVA tumors into total, PD-1$^-$, and PD-1$^+$ CD8 T cells and expanded them for 9–10 days. As depicted in Fig. 3A and B, PD-1$^+$ CD8 TILs had a significantly lower expansion capacity than the PD-1$^-$ population. Curiously, during the first 4 days of culture, bulk CD8 TILs showed a fold expansion similar to that of PD-1$^+$ T cells (Fig. 3B), presumably due to the high proportion of PD-1$^+$ cells in fresh TILs (Fig. 2A), and upon day 6, their growth kinetics was comparable with that of PD-1$^-$ cells. Interestingly, upon expansion, cells derived from PD-1$^+$ CD8 TILs showed higher expression of PD-1 than those derived from bulk or PD-1$^-$ CD8 TILs (Fig. 3C).

We reasoned that the presence of PD-1 ligands on feeder cells or activated T cells might hinder the efficient proliferation of PD-1$^+$ TILs (26). To test this, we expanded the PD-1$^+$ TIL subset in the presence of anti-PD-1 blocking mAb. The blockade of PD-1 during the culture did not enhance the expansion of PD-1$^+$ TILs (Fig. 3D). Similar results were obtained in the presence of anti-PDL-1 mAb (10F.9G2; data not shown). Two different anti-PD-1 mAb clones (HA2-7B1 and 29F.1A12) were used to isolate PD-1$^+$ TILs throughout this study giving comparable results (Fig. 3E).

An important feature of PD-1$^+$ CD8 TILs is that most of them show a TEM phenotype, whereas PD-1$^-$ CD8 TILs are largely central memory T cells (TCM; Fig. 1E). To know whether PD-1$^+$ TILs expand less efficiently due to their TEM differentiation state, we sorted PD-1$^+$ CD8 TILs into PD-1$^+$/CD62L$^+$ and PD-1$^+$/CD62L$^-$ (Fig. 3F). Interestingly, whereas PD-1$^+$/CD62L$^+$ TILs grew nearly as efficiently as PD-1$^-$ cells, PD-1$^+$/CD62L$^-$ cells expanded 10 times less than their counterparts (Fig. 3G). These data indicate that in PD-1$^+$ CD8 TILs is the TEM differentiation state and not the expression of PD-1

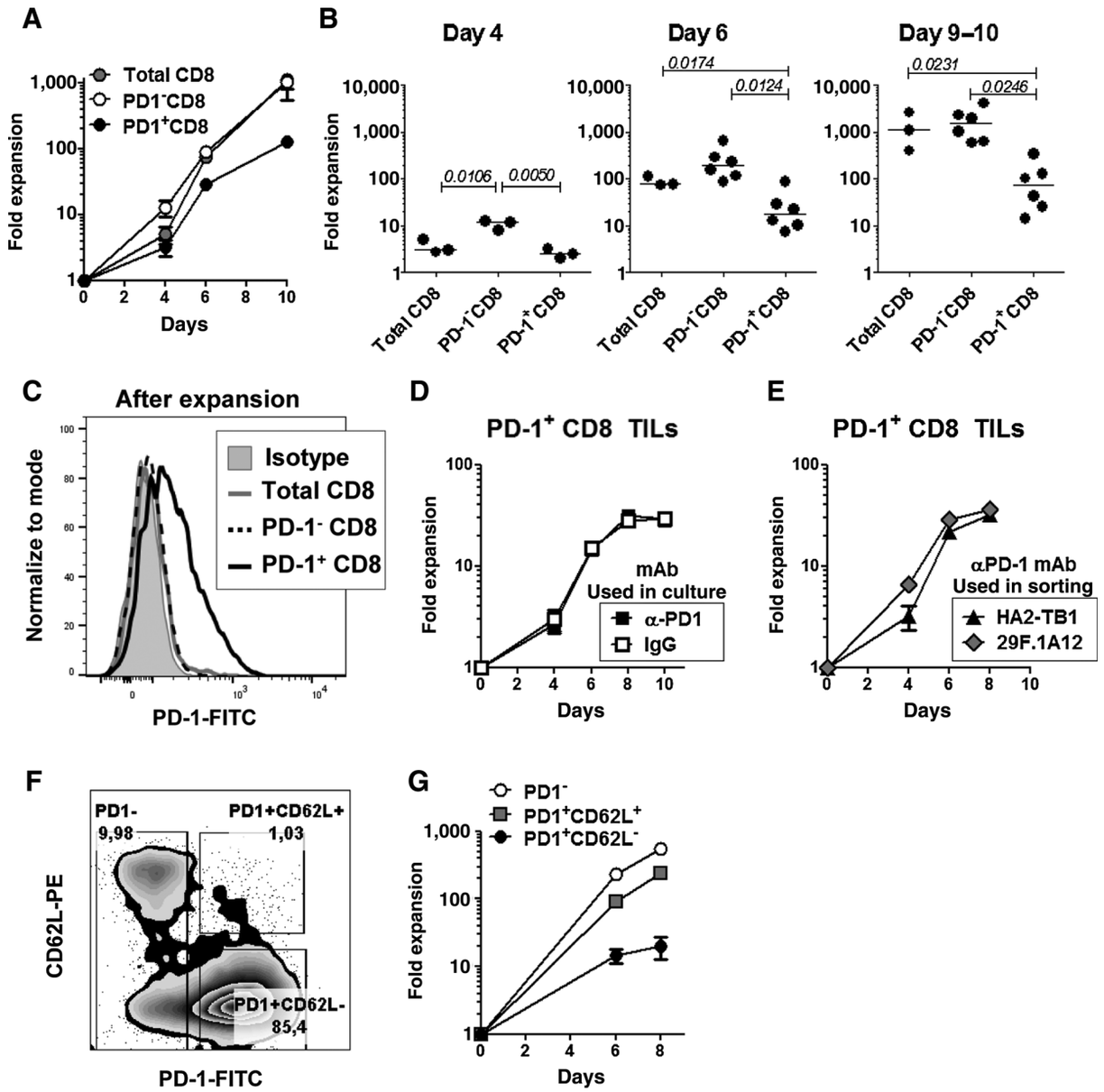

Figure 3.

Kinetics of expansion of different CD8 TIL subsets isolated from B16OVA tumors. **A–D,** Cellular suspension obtained from 15-day sc B16OVA tumors was sorted into total, PD-1$^-$, and PD-1$^+$ CD8 T cells. Isolated cells were expanded in the presence of irradiated feeders cells and anti-CD3 mAbs. **A,** Kinetics of expansion of total, PD-1$^-$, and PD-1$^+$ CD8 TILs. **B,** Fold expansion at day 4 (left), day 6 (center), and day 9–10 (right) of culture. Data compiled from 6 different experiments. Numbers in italics indicate *P* values obtained by unpaired *t* test. **C,** Expression of PD-1 in T cells derived from total, PD-1$^-$, and PD-1$^+$ CD8 TILs at day 9 of expansion. **D,** Kinetics of expansion of PD-1$^+$ CD8 TILs in the presence of anti-PD-1 blocking mAbs or rat IgG along the culture. **E,** Kinetics of expansion of PD-1$^+$ CD8 TILs sorted either with anti-PD-1 mAbs clone HA2-7B1 or with clone 29F.1A12. **F,** Dot plots showing relative expression of PD-1 and CD62L on CD8 TILs. **G,** Kinetics of expansion of PD-1$^-$, PD-1$^+$CD62L$^+$, and PD-1$^+$CD62L$^-$ CD8 TILs. **A**, **B**, **D**, and **G,** Fold expansion was calculated as the output:input ratio of the absolute numbers of cells. **A**, **D**, **E**, and **G,** Mean ± SD of 2–3 culture replicates (each population was divided into 2–3 cultures dishes and cells from each culture dish were counted at the time indicated). One experiment representative of at least six (**A–C**) or two (**D–G**) experiments is shown.

that hampers the *ex vivo* amplification. Similar data were obtained in the mouse model of liver metastasis from colorectal cancer (Supplementary Fig. S4A–S4C). PD-1$^+$/CD137$^-$ and PD-1$^+$/CD137$^+$ CD8 TILs from both tumor models showed similar expansion kinetics *ex vivo* (Supplementary Fig. S3B and S3E).

PD-1$^+$ CD8 TILs, rather than total CD8 TILs, more faithfully maintain the repertoire of tumor-specific TCRs after *in vitro* expansion

Next, we compared the percentage of tetramer$^+$ cells in each CD8 TIL population before and after expansion. Interestingly, whereas OVA- and M8-specific T cells were still prominent within

the T-cell product derived from PD-1$^+$ cells, they became imperceptible in those cells expanded from bulk CD8 TILs (Fig. 4).

Curiously, in the PD-1$^+$ CD8 T-cell subset, the frequency of M8-tetramer$^+$ cells significantly decreased after expansion, while the percentage of OVA-specific T cells was not seriously affected (Fig. 4B). This finding suggested that during the expansion phase the TCR repertoire of PD-1$^+$ CD8 TILs has also probably changed. To investigate in more detail a potential TCR bias produced along the culture, we analyzed the length of the CDR3 regions from 22 Vβ families in the different TIL subsets before and after expansion.

The spectratype analysis of freshly isolated PD-1$^-$ CD8 TILs revealed a Gaussian profile indicative of a polyclonal repertoire (27), and this normal distribution was maintained after expansion (Supplementary Fig. S5). In contrast, PD-1$^+$ CD8 TILs exhibited one or a limited number of CDR3 sizes (fragments/peaks) in several Vβ families, indicative of T cells that have experienced Ag-driven clonal expansion. In addition, the spectratype profiles of freshly isolated PD-1$^+$ and total CD8 TILs were very similar showing multiple TCR-Vβ usages typical of a heterogeneous population. The original TCR repertoire was better conserved in the T-cell product derived from PD-1$^+$ CD8 TILs than in that obtained from total CD8 TILs (Supplementary Fig. S5; Supplementary Table S1). Thus, some dominant peaks were conserved after expansion (labeled with an orange asterisk; Supplementary Fig. S5) and this phenomenon was more apparent in PD-1$^+$ than in total CD8 TILs (Supplementary Table S1). Accordingly, the number of Vβ families that maintained some of the originally dominant CDR3 fragments after expansion was higher in PD-1$^+$ (12/22 in experiment 1, and 13/22 in experiment 2) than in total CD8 TILs (5/22 and 8/22, in experiment 1 and 2, respectively; Supplementary Table S2).

Although, in general, the TCR repertoire was more reliably preserved in cells derived from PD-1$^+$ TILs, we also observed important changes in the TCR spectratyping profile of this subset after expansion. Indeed, many dominant CDR3 fragments in the starting TIL populations completely disappeared after expansion (labeled with a blue asterisk), whereas others that were either initially undetected or present at a very low level became leaders in

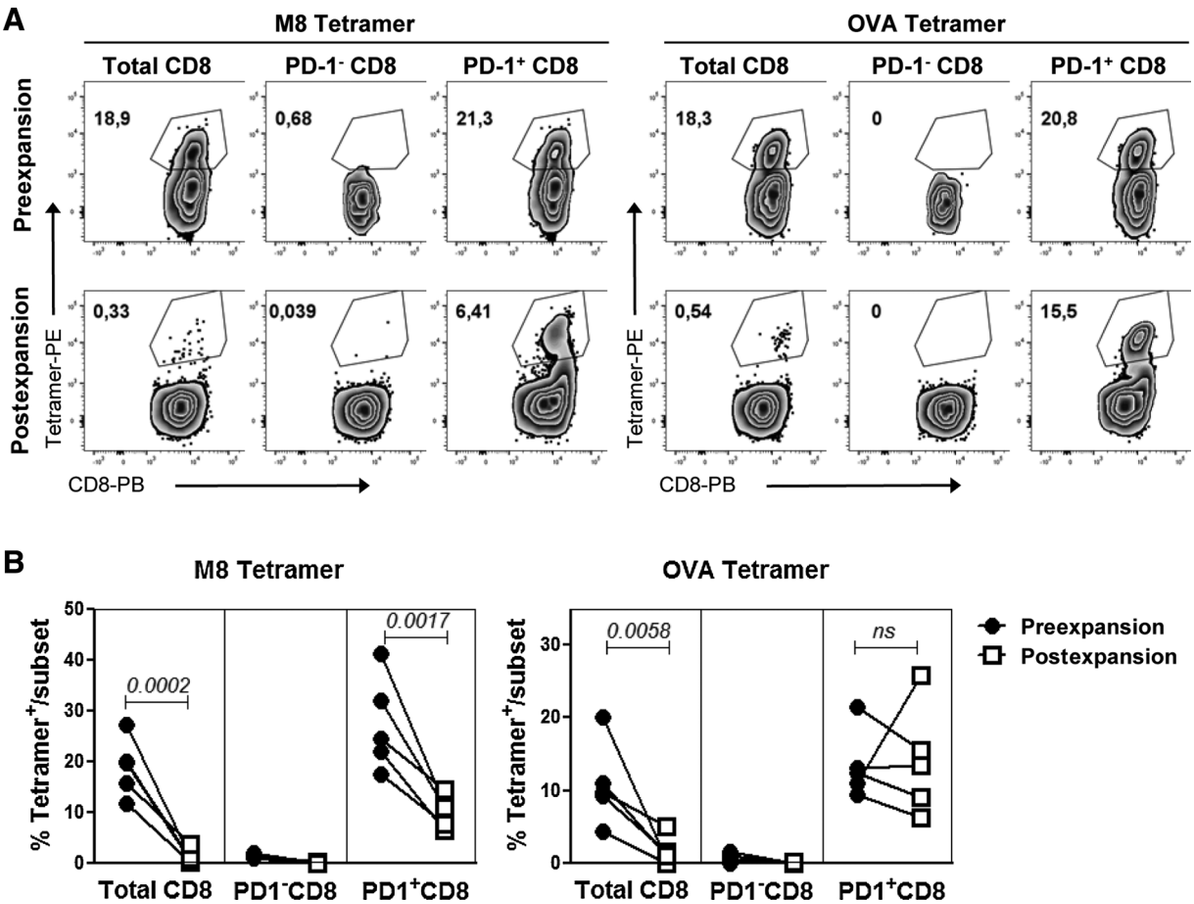

Figure 4.

Percentage of Tetramer$^+$ cells in different CD8 TIL subsets before and after *in vitro* expansion. **A** and **B,** To estimate the frequency of Tetramer$^+$ cells before expansion, total tumor cell suspension was stained with tetramers and mAbs and cells were gated as "Total CD8$^+$," "PD-1$^-$CD8$^+$," and "PD-1$^+$CD8$^+$" by flow cytometry. The frequency of tetramer$^+$ cells within these populations is shown. To assess the percentage of Tetramer$^+$ cells after expansion, CD8 TIL subsets were isolated on the basis of PD-1 expression and expanded as in Fig. 3. At day 9–10 of culture, cells were stained with tetramers and mAbs and analyzed by flow cytometry. **A,** A representative experiment showing the frequency of M8- and OVA-tetramer$^+$ cells in different CD8 T-cell subsets before (pre-) and after (post-) expansion. **B,** Data compiled from five different experiments. Numbers in italics indicate *P* values obtained by unpaired *t* test.

the final T-cell product (green asterisk; Supplementary Fig. S5; Supplementary Table S1). Similar data were found in the other two TIL subsets.

Collectively, these data indicate that despite the interclonal competition during the expansion process, PD-1$^+$ TILs, rather than total CD8 TILs, more faithfully maintain the TCR repertoire after *in vitro* culture.

Cells expanded from the PD-1$^+$ compartment, but not from bulk CD8 TILs, maintained their ability to recognize tumor cells

To investigate whether tumor specificity was maintained upon *in vitro* expansion, T-cell products derived from bulk, PD-1$^-$, and PD-1$^+$ CD8 TILs were tested for reactivity against the related tumor cell line (B16OVA) in a standard coculture assay. T cells derived from PD-1$^+$ CD8 TILs, but not those expanded from total CD8 TILs or from the PD-1$^-$ compartment, showed reactivity to B16OVA cells, as determined by IFN-γ-ELISPOT assay (Fig. 5A) and CD137 upregulation (Fig. 5B). The response of PD-1$^+$ derived T cells was Ag-driven as they did not respond to the unrelated ID8 tumor cell line (Fig. 5A and B). No tumor reactivity was detected against other unrelated cell lines, such as EL4 (data not shown). We only detected reactivity when the unrelated cell lines shared some antigen with B16OVA cells (as is the case with the M8 antigen in the MC38 cell line, and OVA antigen in the EG7 cell line; data not shown). We also compared the tumor reactivity of PD-1$^+$/CD62L$^+$ versus PD-1$^+$/CD62L$^-$ cells and of PD-1$^+$/CD137$^+$ versus PD-1$^+$/CD137$^-$ cells after expansion. All subsets specifically recognized B16OVA cells (Fig. 5C; Supplementary Fig. S3C). The tumor reactivity of PD-1$^+$–derived cells (whether or not they expressed CD62L or CD137) was also confirmed in the MC38 mouse model (Supplementary Figs. S3F and S4D and S4E).

PD-1 precisely identifies marrow-infiltrating tumor-specific CD8 T cells in multiple myeloma–bearing mice

We also explored the capacity of PD-1 to isolate tumor-specific T cells in a mouse model of multiple myeloma based on 5TGM1 cell line. Five to seven weeks after the intravenous injection of 5TGM1-GFP cells, mice developed multiple myeloma, as detected by the increased levels of IgG2bκ paraprotein in the sera (Fig. 6A) and the hind-limb paralysis. Tumor cells (GFP$^+$) were detected in the bone marrow and in the spleen of multiple myeloma–bearing mice with a notably greater tumor burden in bone marrow (Fig. 6B, top). Importantly, PD-1$^+$ CD8 T cells were detected in both tissues being more prevalent in bone marrow (Fig. 6B, bottom and C). A small proportion of PD-1$^-$ and PD-1$^+$ CD8 T cells from multiple myeloma–bearing mice also expressed CD137.

The bone marrow is the niche for multiple myeloma, but also is a site for the priming of naïve T cells and the maintenance of memory T cells (28, 29). Therefore, the selection of the right CD8 T-cell subset is especially important to implement TIL therapy for the treatment of multiple myeloma. To compare the ability of

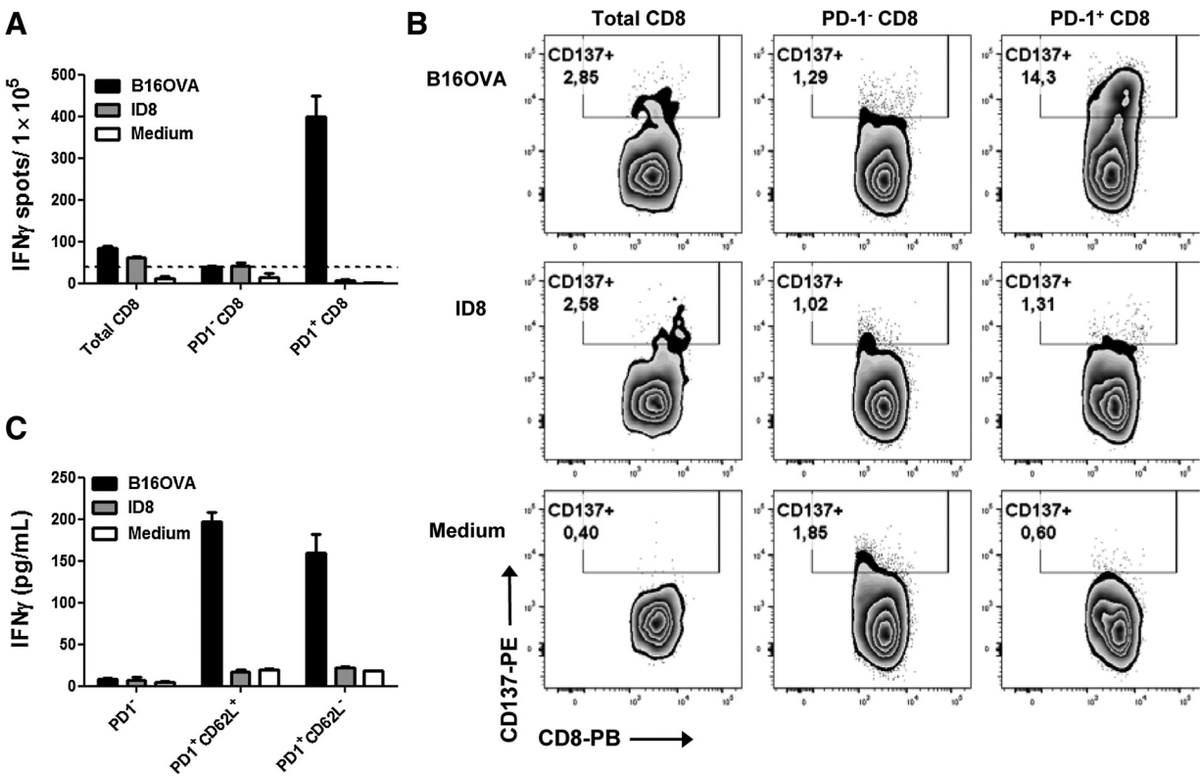

Figure 5.

Tumor reactivity of T-cell products derived from different CD8 TIL subset isolated on the basis of PD-1 expression. **A–C,** Cells expanded from the indicated CD8 TIL subsets isolated from subcutaneous B16OVA tumors were cultured with B16OVA and unrelated (ID8) tumor cells and tumor reactivity was assessed by measuring IFNγ production [ELISPOT (**A**) or ELISA (**C**)] or CD137 upregulation (**B**). **A,** Dotted vertical line indicates threshold value (40 spots). **A** and **C,** Mean ± SD of three culture replicates. One experiment representative of at least 6 (n = 4–5/experiment; **A** and **B**) or two (n = 4/experiment; **C**) experiments.

CD137 and PD-1 to isolate myeloma-reactive T cells, bone marrow cells and splenocytes from multiple myeloma–bearing mice were sorted into PD-1$^-$/CD137$^-$, PD-1$^-$/CD137$^+$, PD-1$^+$/CD137$^-$ and PD-1$^+$/CD137$^+$ CD8 T cells. As occurred in the solid tumor models, the fold expansion of PD-1$^+$ CD8 T cells was lower than that of PD-1$^-$ cells (Fig. 6D). Interestingly, only those cells derived from the marrow-infiltrating PD-1$^+$ subsets (whether or not they expressed CD137), but no cells derived from the splenic populations, were able to specifically recognize parental 5TGM1 cells (Fig. 6E). These data indicate that in high tumor-burden tissue, as is the case of bone marrow in multiple myeloma–bearing mice, PD-1 precisely identified myeloma-specific T cells. Interestingly, the PD-1$^-$/CD137$^+$ cells expanded more efficiently than PD-1$^+$/CD137$^+$ population (Fig. 6D), but they did not recognize tumor cells (Fig. 6E and F). Therefore, if CD137 was used as single marker for the sorting, the PD-1$^-$ subset within CD137$^+$ cells would overgrow PD-1$^+$/CD137$^+$ cells diluting the tumor reactivity of the final cellular products. To sum-up, PD-1, rather than CD137, more precisely and comprehensively identified myeloma-specific T cells within the marrow-infiltrating CD8 T cells.

Enrichment and separate expansion of PD-1$^+$ CD8 TILs improve the efficacy of TIL therapy

To investigate the therapeutic potential of PD-1-selected CD8 TILs, we first explored the use of TILs in the treatment of mice with established pulmonary micrometastases. Three days after the intravenous injection of B16OVA or MC38 tumor cells, mice were treated with 2×10^6 cells expanded from PD-1$^-$ or PD-1$^+$ CD8 TILs. The adoptive transfer of PD-1$^+$ TILs but not of PD-1$^-$ cells improved the survival in both micrometastasis models (Fig. 7A and B).

We next explored the treatment of large established tumors. Mice bearing 6-day or 10-day subcutaneous B16OVA tumors received a sublethal dose of TBI and were then treated with 10^7 cells expanded from total, PD-1$^-$ and PD-1$^+$ CD8 TILs. As shown in Fig. 7C and D, the ACT of PD-1$^+$ TILs notably delayed tumor growth and enhanced survival of mice bearing 6-day established tumors, compared with the use of total or PD-1$^-$ CD8 TILs. However, in the 10-day established tumor setting, the treatment with PD-1$^+$ TILs had a very slight impact (Fig. 7E and F). As PD-1$^+$ TILs maintain a relatively high expression of PD-1 after expansion (Fig. 3H), we reasoned that the combination of ACT with PD-1/PDL-1 blockade may have improved their efficacy in large established tumors. Thus, mice bearing 10-day tumors were treated as before and the day after ACT they received a single injection of anti-PDL-1 blocking mAbs. As a control, groups of mice received anti-PDL-1, either with or without previous TBI. As depicted in Fig. 7E and F, treatment with anti-PDL-1 alone had no impact on B16OVA tumors. Interestingly the antitumor efficacy of anti-PDL-1 was higher in those mice that were previously irradiated, probably due to the TBI-mediated depletion of endogenous Tregs and enhancement of tumor-Ag presentation (30). Importantly, the therapeutic benefit of PD-1$^+$ TILs in large established tumor was substantially enhanced by the anti-PDL-1 blockade.

Discussion

Recently, several studies in melanoma patients have found that most antitumor reactivity is harbored by the PD-1$^+$ CD8 TIL subset (17, 18). This discovery suggests that the T-cell product derived from PD-1$^+$ CD8 TILs can be used for infusion in ACT schedules. However, to date no study has addressed the *in vivo* antitumor activity of PD-1–selected TILs. Using two different mouse models of solid tumors, we have demonstrated that the enrichment and separate amplification of PD-1$^+$ CD8 TILs improves the antitumor efficacy of TIL therapy. In addition, we show that PD-1 precisely identifies marrow-infiltrating tumor-specific CD8 T cells in multiple myeloma–bearing mice, revealing a way to implement TIL therapy for the treatment of hematologic tumors. Our data provide a rationale for the use of PD-1 to select tumor-specific T cells for the development of TIL therapies.

The mouse models of melanoma and colon adenocarcinoma used in this study are characterized by a high proportion of CD8 TILs expressing PD-1 (70%–90%). In these models, highly immunodominant tumor-specific CD8 TILs, identified by tetramer staining, were almost exclusively assigned to the PD-1$^+$ compartment. In addition, PD-1 in the fresh tumor can be used to identify and isolate the full repertoire of tumor-reactive CD8 TILs without requiring knowledge of their Ag specificities. Interestingly, PD-1 also supports the isolation of marrow-infiltrating tumor-specific T cells in a mouse model of multiple myeloma. Therefore, PD-1 may evolve as a biomarker for the isolation of naturally occurring tumor-reactive T cells in large panels of tumor types.

Surprisingly, despite the high proportion of tumor-reactive T cells present in bulk CD8 TILs before expansion, only T cells expanded from PD-1–selected CD8 TILs, but not those from bulk CD8 TILs, were able to specifically recognize tumor cells. Interestingly, the fold expansion of PD-1$^+$ CD8 TILs was 10 times lower than that of PD-1$^-$ cells. This may explain the lack of tumor reactivity of the T-cell product obtained from bulk CD8 TILs, as, during the expansion, cells derived from the minority PD-1$^-$ subset may have exceeded in number those coming from the initially main population (PD-1$^+$). This, together with the bystander nature of PD-1$^-$ TILs, highlights the importance of separately expanding PD-1$^+$ CD8 TILs to obtain T-cell products with high antitumor activity.

The reasons why PD-1$^+$ CD8 T cells expand less than PD-1$^-$ T cells are being currently investigated by our group. The use of blocking mAbs against PD-1 or PDL-1 during culture did not enhance the expansion of PD-1$^+$ TILs, meaning that the plausible expression of PD-1 ligands on feeder cells or activated T cells does not affect the expansion of PD-1$^+$ TILs (26). However, as PD-1$^+$ TILs also express inhibitor receptors, such as LAG-3 and CTLA-4, we cannot rule out the possibility that other inhibitory signals may be impairing the expansion of this TIL subset. An important feature of tumor-infiltrating PD-1$^+$ T cells is that most of them show a TEM phenotype, whereas PD-1$^-$ TILs are largely TCM. TEM T cells exhibit lower proliferative capacity upon TCR triggering than their TCM counterparts (31–33). Interestingly, CD62L$^+$/PD-1$^+$ TILs expanded 8–10 times more than CD62L$^-$/PD-1$^+$ cells, suggesting that the predominant TEM differentiation state of PD-1$^+$ CD8 TILs, and not the expression of PD-1 or other inhibitory receptors, is the main factor that hampers the *ex vivo* expansion of this subset.

The frequencies of well-defined tumor-specific T-cell populations, as determined by tetramer staining, together with the analysis of the CDR3 spectratyping profile before and after expansion, revealed that the original TCR repertoire was more faithfully preserved in the T-cell product derived from PD-1$^+$ CD8 TILs than in that obtained from total CD8 TILs. Nevertheless, the peak

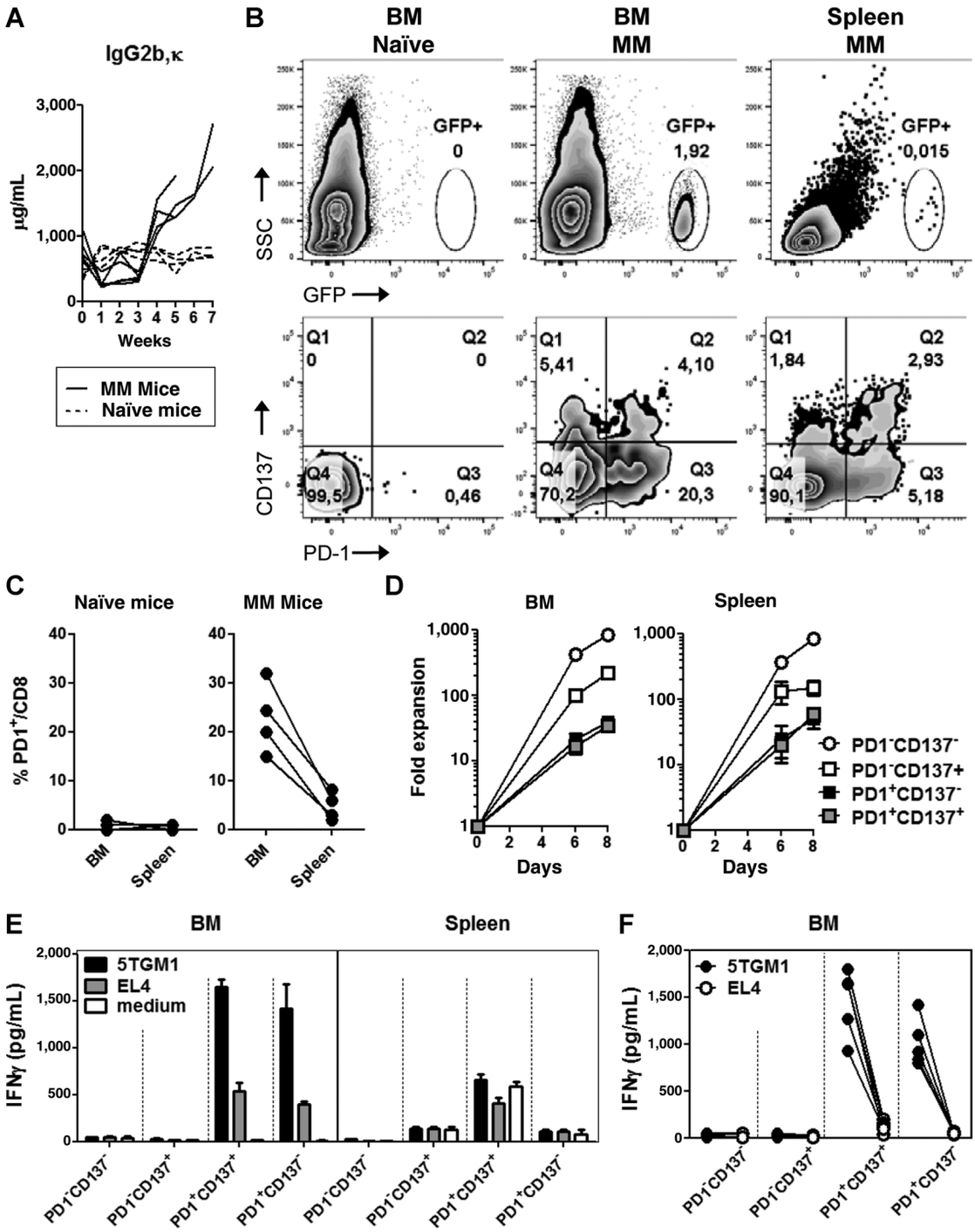

Figure 6.

PD-1, rather than CD137, precisely identifies bone marrow–infiltrating tumor-specific CD8 T cells in multiple myeloma (MM)-bearing mice. 5TGM1-GFP cells were injected intravenously into C57BL/K mice. When the mice showed the first symptoms of illness and the IgG2bκ paraprotein was detected in the sera, animals were sacrificed and splenocytes and bone marrow (BM) cells were analyzed. **A,** Levels of seric IgG2bκ paraprotein detected by ELISA. **B,** Dot plots show the presence of tumor cells (GFP^+; top) and the expression of PD-1 and CD137 (bottom) by splenic and marrow-infiltrating CD8 T cells from a representative multiple myeloma–bearing mouse. As a comparison, bone marrow cells from a naïve mouse are also shown. Top and bottom panels were gated on total live cells and live $CD8^+$ cells, respectively. **C,** Frequency of $PD\text{-}1^+$ cells within the marrow-infiltrating CD8 T-cell population in naïve versus multiple myeloma–bearing mice. **D** and **E,** Splenic and bone marrow cells from multiple myeloma–bearing mice were sorted into $PD\text{-}1^-CD137^+$, $PD\text{-}1^+CD137^-$, $PD\text{-}1^+CD137^+$, and $PD\text{-}1^-CD137^-$ CD8 T cells and expanded as before. **D,** Kinetics of expansion of splenic and marrow-infiltrating CD8 T-cell subsets. **E** and **F,** After expansion, cells derived from those isolated from bone marrow or spleen were cultured with parental 5TGM1 (nonexpressing GFP) and unrelated tumor cells (EL4), and tumor reactivity was assessed by measuring IFNγ production by ELISA. One mice representative of five (**E**) and compiled data from 5 different mice (**F**). **D** and **E,** The mean ± SD (three culture replicates) is plotted.

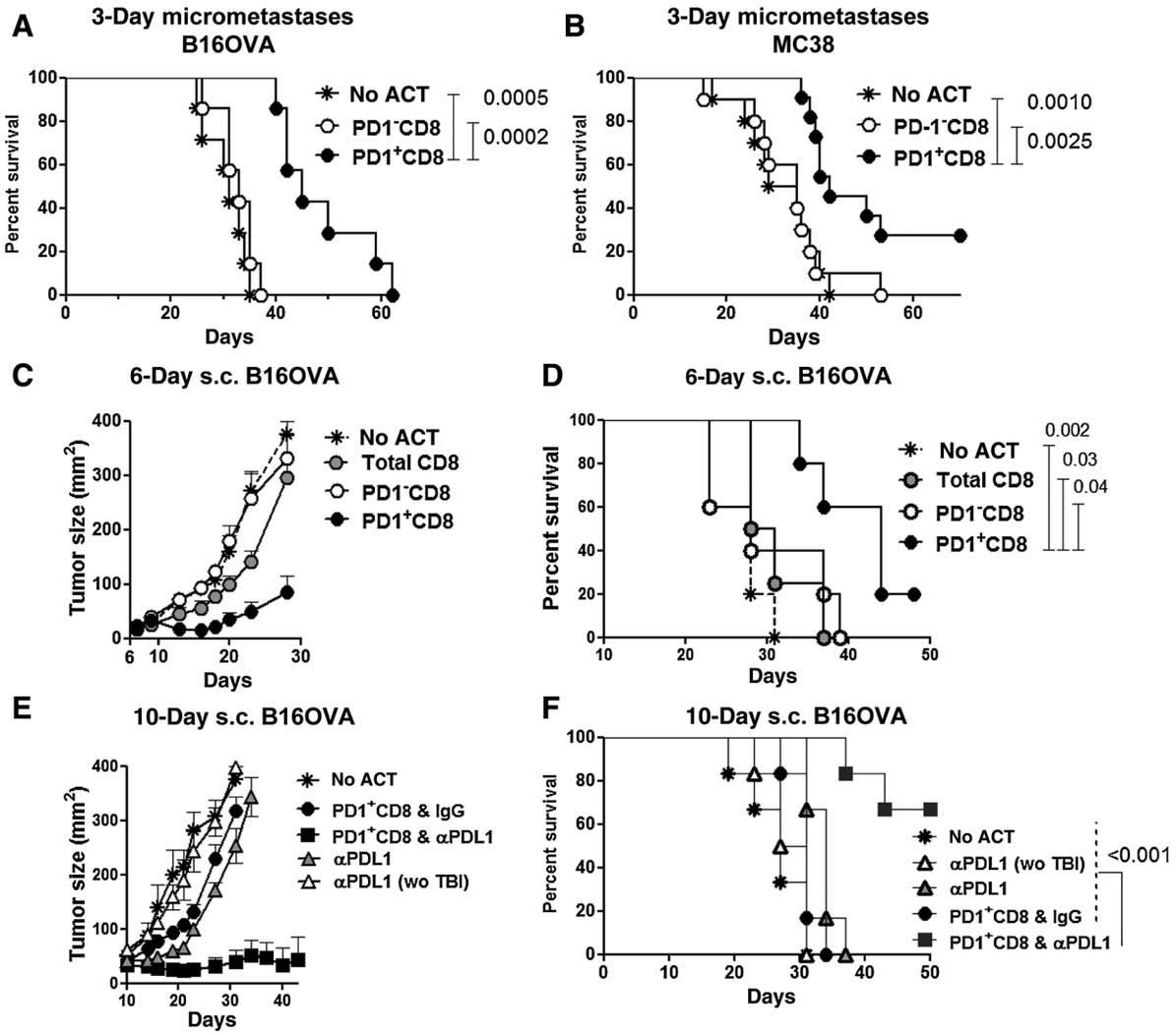

Figure 7.

Enrichment and separate expansion of PD-1$^+$ CD8 TILs improves the efficacy of TIL therapy. **A** and **B,** Model of melanoma and colon adenocarcinoma micrometastases. B16OVA or MC38 tumor cells (5×10^5) were injected intravenously into BL6 mice and 3 days later therapy was instituted with 2×10^6 TILs obtained from 15-day subcutaneous (s.c.) B16OVA or 15-day intrahepatic MC38 tumors, respectively, or without TILs (no ACT) in combination with systemic administration of IL2. **C–F,** Mouse model of large established melanoma tumors. BL6 mice were injected subcutaneously with 5×10^5 B16OVA tumor cells. Mice bearing 6-day (**C** and **D**) or 10-day (**E** and **F**) tumors were irradiated and therapy was instituted with 10^7 TILs obtained from 15-day subcutaneous B16OVA tumors or without TILs (no ACT) and IL2 as before. The day after ACT some mice received a single injection of anti-PDL-1 mAbs (**E** and **F**). As a control, groups of mice received anti-PDL-1 and IL2, either with or without previous TBI (**E** and **F**). Antitumor efficacy was assessed by monitoring mice survival (**A**, **B**, **D**, and **F**) and tumor growth (**C** and **E**). The tumor size is represented as the product of the two perpendicular diameters (median ± SEM). Asterisks show statistical significance by Bonferroni multiple comparison (**C** and **E**) and log rank (**A**, **B**, **D**, and **F**) tests. Each panel is one experiment representative of at least two experiments.

profile of most of the TCR-Vβ families from the PD-1$^+$ subset also substantially changes after expansion. Indeed, many dominant CDR3 fragments in the starting TIL population completely disappeared after the *ex vivo* expansion, whereas others that were either initially undetected or present at a very low level (subdominant) became leaders in the final T-cell product. Similar data have been reported by Rosenberg and colleagues in human TILs (34). These findings indicate that the *in vitro* expansion resulted in preferential expansion of subdominant clones in the original sample probably coming from less differentiated T cells, such as the CD62L$^+$/PD-1$^+$ CD8 TIL subset. The low number of these cells in the starting sample difficult further studies.

Our data have important implications for the commercialization of TIL therapy. PD-1$^+$ CD8 T cells can be easily and rapidly isolated using FACS or magnetic technologies. The use of preenriched tumor-specific T cells may simplify the TIL production method by circumventing the tumor fragment culture that precedes the expansion phase. Importantly, our study shows that separate expansion of PD-1$^+$ TILs generates T-cell products with higher predictable antitumor activity. On the other hand, the current culture technology has generally been incapable of generating TILs with tumor reactivity in patients with nonmelanoma solid malignancies (35), probably due to the lower frequency of tumor-reactive T lymphocytes (in contrast to melanoma). PD-1

may enable the isolation of rare tumor-specific TILs and allow TIL therapy to be extended to tumor types other than melanoma.

Recently, in an effort to extend the ACT with natural tumor-specific T cells to the treatment of multiple myeloma, Borrello and colleagues have developed the use of marrow-infiltrating lymphocytes (MIL; ref. 36). In a previous study, they showed that cells expanded *ex vivo* from MILs, but not those from peripheral blood lymphocytes, recognize autologous myeloma cells (37), indicating that the bone marrow represents a unique site to obtain myeloma-specific T cells. The Johns Hopkins team has recently carried out a pilot clinical study in multiple myeloma patients using cells expanded from bulk MILs (36). Thirteen of the 22 patients treated experienced some tumor load reduction. Interestingly, the authors observed a direct correlation between the tumor specificity of the *ex vivo*–expanded MILs with clinical outcomes (36). Although such results hold promise, the clinical benefit of the MIL therapy is still modest. Possible contamination of MIL products with T cells unrelated to tumors may likely have diminished the efficacy of the MIL therapy. Our findings in the murine 5TGM1 model highlight the importance of expanding the right CD8 T-cell population to obtain a final MIL product with high tumor specificity.

Lately, some controversy has arisen regarding which molecule, PD-1 or CD137, better identifies the tumor-specific CD8 TIL population (13, 18). Interestingly, in the three mouse models studied here, we could only detected tumor-reactive cells in the PD-1^+/CD137^+ and PD-1^+/CD137^- TIL/MIL populations, indicating that both molecules, PD-1 and CD137, can be used to enrich tumor-reactive T cells. However, the findings that (i) a significant fraction of tumor-specific T cells was found in the PD-1^+/CD137^- TIL/MIL compartment, and that (ii) PD-1^-/CD137^+ CD8 MILs from multiple myeloma–bearing mice were not tumor-specific, clearly show that PD-1, rather than CD137, more precisely and comprehensively identifies tumor-specific CD8 T cells.

One of the major challenges for TIL therapy now is the rapidly developing field of the checkpoint blockade (38). TIL therapy will not most likely be a standalone therapy but will need to be part of a larger combination regimen with checkpoint inhibitors. The need to perform this combination may be also critical when using PD-1-selected TILs, given the fact that these cells maintain a relatively high expression of PD-1 after expansion. As we showed in the current study, the combined administration of anti-PDL-1 mAbs with PD-1^+ TILs was critical in the treatment of large established tumor. Therefore, TIL therapy may become an excellent synergistic treatment with checkpoint blockade in patients with progressive disease after checkpoint inhibitors, especially in nonmelanoma indications, where response rates are still low (39, 40).

Disclosure of Potential Conflicts of Interest

No potential conflicts of interest were disclosed.

Authors' Contributions

Conception and design: D. Salas-Benito, S. Hervas-Stubbs
Development of methodology: S.M. Fernandez-Poma, T. Lozano, N. Casares, J.-I. Riezu-Boj, U. Mancheño, E. Elizalde, N. Zubeldia, E. Conde
Acquisition of data (provided animals, acquired and managed patients, provided facilities, etc.): S.M. Fernandez-Poma, D. Salas-Benito, N. Casares, D. Alignani, I. Otano
Analysis and interpretation of data (e.g., statistical analysis, biostatistics, computational analysis): S.M. Fernandez-Poma, D. Salas-Benito, P. Sarobe, J.J. Lasarte, S. Hervas-Stubbs
Writing, review, and/or revision of the manuscript: N. Casares, I. Otano, P. Sarobe, J.J. Lasarte, S. Hervas-Stubbs
Administrative, technical, or material support (i.e., reporting or organizing data, constructing databases): U. Mancheño, E. Elizalde, N. Zubeldia, E. Conde, J.J. Lasarte
Study supervision: J.J. Lasarte, S. Hervas-Stubbs
Other (performed experiments in B16OVA and MC38 mouse models): S.M. Fernandez-Poma, U. Mancheño, E. Elizalde, N. Zubeldia, E. Conde
Other (developed spectratyping technology): J.-I. Riezu-Boj
Other (provided the original ideas, directed the study, analysed the data and wrote the final version of the paper): S. Hervas-Stubbs

Acknowledgments

Authors thank Drs. I. Melero, K. Roby, and B.O. Oyajobi for the kind gift of cell lines and I. Rodriguez from the Flow Cytometry Unit (CIMA) for her help with flow cytometry studies. Members of animal facility and Genomics Unit at CIMA are also acknowledged.

Grant Support

This work was supported by Ministerio de Eduación from Peru [Programa Nacional de Becas y Crédito Educativo (PRONABEC), Beca Presidente de la República to S.M. Fernandez-Poma], by Ministerio de Economía y Competitividad (SAF2013-42772-R and SAF2016-78568-R to J.J. Lasarte), and Instituto de Salud Carlos III (PI15/02027 to S. Hervas-Stubbs) from Spain and by Fundación Ramón y Areces (grant to E.Conde, S. Hervas-Stubbs, and J.J. Lasarte).

The costs of publication of this article were defrayed in part by the payment of page charges. This article must therefore be hereby marked *advertisement* in accordance with 18 U.S.C. Section 1734 solely to indicate this fact.

Received January 24, 2017; revised April 6, 2017; accepted May 1, 2017; published OnlineFirst May 18, 2017.

References

1. Rosenberg SA, Restifo NP. Adoptive cell transfer as personalized immunotherapy for human cancer. Science 2015;348:62–8.
2. Radvanyi LG. Tumor-infiltrating lymphocyte therapy: addressing prevailing questions. Cancer J 2015;21:450–64.
3. Pasetto A, Gros A, Robbins PF, Deniger DC, Prickett TD, Matus-Nicodemos R, et al. Tumor- and neoantigen-reactive T-cell receptors can be identified based on their frequency in fresh tumor. Cancer Immunol Res 2016;4:734–43.
4. Barrett DM, Grupp SA, June CH. Chimeric antigen receptor- and TCR-modified T cells enter main street and wall street. J Immunol 2015; 195:755–61.
5. Gros A, Parkhurst MR, Tran E, Pasetto A, Robbins PF, Ilyas S, et al. Prospective identification of neoantigen-specific lymphocytes in the peripheral blood of melanoma patients. Nat Med 2016;22:433–8.
6. Dudley ME, Wunderlich JR, Shelton TE, Even J, Rosenberg SA. Generation of tumor-infiltrating lymphocyte cultures for use in adoptive transfer therapy for melanoma patients. J Immunother 2003;26:332–42.
7. Rosenberg SA, Yang JC, Sherry RM, Kammula US, Hughes MS, Phan GQ, et al. Durable complete responses in heavily pretreated patients with metastatic melanoma using T-cell transfer immunotherapy. Clin Cancer Res 2011;17:4550–7.
8. Besser MJ, Shapira-Frommer R, Treves AJ, Zippel D, Itzhaki O, Schallmach E, et al. Minimally cultured or selected autologous tumor-infiltrating lymphocytes after a lympho-depleting chemotherapy regimen in metastatic melanoma patients. J Immunother 2009; 32:415–23.
9. Besser MJ, Shapira-Frommer R, Treves AJ, Zippel D, Itzhaki O, Hershkovitz L, et al. Clinical responses in a phase II study using adoptive transfer of

short-term cultured tumor infiltration lymphocytes in metastatic melanoma patients. Clin Cancer Res 2010;16:2646–55.
10. Besser MJ, Shapira-Frommer R, Itzhaki O, Treves AJ, Zippel DB, Levy D, et al. Adoptive transfer of tumor-infiltrating lymphocytes in patients with metastatic melanoma: intent-to-treat analysis and efficacy after failure to prior immunotherapies. Clin Cancer Res 2013;19:4792–800.
11. Croft M. The role of TNF superfamily members in T-cell function and diseases. Nat Rev Immunol 2009;9:271–85.
12. Wolfl M, Kuball J, Ho WY, Nguyen H, Manley TJ, Bleakley M, et al. Activation-induced expression of CD137 permits detection, isolation, and expansion of the full repertoire of CD8+ T cells responding to antigen without requiring knowledge of epitope specificities. Blood 2007;110: 201–10.
13. Ye Q, Song DG, Poussin M, Yamamoto T, Best A, Li C, et al. CD137 accurately identifies and enriches for naturally occurring tumor-reactive T cells in tumor. Clin Cancer Res 2014;20:44–55.
14. Sauce D, Almeida JR, Larsen M, Haro L, Autran B, Freeman GJ, et al. PD-1 expression on human CD8 T cells depends on both state of differentiation and activation status. AIDS 2007;21:2005–13.
15. Ahmadzadeh M, Johnson LA, Heemskerk B, Wunderlich JR, Dudley ME, White DE, et al. Tumor antigen-specific CD8 T cells infiltrating the tumor express high levels of PD-1 and are functionally impaired. Blood 2009;114:1537–44.
16. Baitsch L, Baumgaertner P, Devevre E, Raghav SK, Legat A, Barba L, et al. Exhaustion of tumor-specific CD8(+) T cells in metastases from melanoma patients. J Clin Invest 2011;121:2350–60.
17. Inozume T, Hanada K, Wang QJ, Ahmadzadeh M, Wunderlich JR, Rosenberg SA, et al. Selection of CD8+PD-1+ lymphocytes in fresh human melanomas enriches for tumor-reactive T cells. J Immunother 2010; 33:956–64.
18. Gros A, Robbins PF, Yao X, Li YF, Turcotte S, Tran E, et al. PD-1 identifies the patient-specific CD8(+) tumor-reactive repertoire infiltrating human tumors. J Clin Invest 2014;124:2246–59.
19. Rosenberg SA, Spiess P, Lafreniere R. A new approach to the adoptive immunotherapy of cancer with tumor-infiltrating lymphocytes. Science 1986;233:1318–21.
20. Mayordomo JI, Zorina T, Storkus WJ, Zitvogel L, Celluzzi C, Falo LD, et al. Bone marrow-derived dendritic cells pulsed with synthetic tumour peptides elicit protective and therapeutic antitumour immunity. Nat Med 1995;1:1297–302.
21. Roby KF, Taylor CC, Sweetwood JP, Cheng Y, Pace JL, Tawfik O, et al. Development of a syngeneic mouse model for events related to ovarian cancer. Carcinogenesis 2000;21:585–91.
22. Radl J, Croese JW, Zurcher C, Van den Enden-Vieveen MH, de Leeuw AM. Animal model of human disease. multiple myeloma. Am J Pathol 1988;132:593–7.
23. Dallas SL, Garrett IR, Oyajobi BO, Dallas MR, Boyce BF, Bauss F, et al. Ibandronate reduces osteolytic lesions but not tumor burden in a murine model of myeloma bone disease. Blood 1999;93:1697–706.
24. Jin C, Yu D, Hillerdal V, Wallgren A, Karlsson-Parra A, Essand M. Allogeneic lymphocyte-licensed DCs expand T cells with improved antitumor activity and resistance to oxidative stress and immunosuppressive factors. Mol Ther Methods Clin Dev 2014;1:14001.
25. Yang CY, Best JA, Knell J, Yang E, Sheridan AD, Jesionek AK, et al. The transcriptional regulators Id2 and Id3 control the formation of distinct memory CD8+ T cell subsets. Nat Immunol 2011;12:1221–9.
26. Patsoukis N, Sari D, Boussiotis VA. PD-1 inhibits T cell proliferation by upregulating p27 and p15 and suppressing Cdc25A. Cell Cycle 2012; 11:4305–9.
27. Pannetier C, Even J, Kourilsky P. T-cell repertoire diversity and clonal expansions in normal and clinical samples. Immunol Today 1995; 16:176–81.
28. Feuerer M, Beckhove P, Garbi N, Mahnke Y, Limmer A, Hommel M, et al. Bone marrow as a priming site for T-cell responses to blood-borne antigen. Nat Med 2003;9:1151–7.
29. Di Rosa F, Santoni A. Bone marrow CD8 T cells are in a different activation state than those in lymphoid periphery. Eur J Immunol 2002;32:1873–80.
30. Klebanoff CA, Khong HT, Antony PA, Palmer DC, Restifo NP. Sinks, suppressors and antigen presenters: how lymphodepletion enhances T cell-mediated tumor immunotherapy. Trends Immunol 2005; 26:111–7.
31. Wherry EJ, Teichgraber V, Becker TC, Masopust D, Kaech SM, Antia R, et al. Lineage relationship and protective immunity of memory CD8 T cell subsets. Nat Immunol 2003;4:225–34.
32. Klebanoff CA, Gattinoni L, Torabi-Parizi P, Kerstann K, Cardones AR, Finkelstein SE, et al. Central memory self/tumor-reactive CD8+ T cells confer superior antitumor immunity compared with effector memory T cells. Proc Natl Acad Sci U S A 2005;102:9571–6.
33. Roberts AD, Ely KH, Woodland DL. Differential contributions of central and effector memory T cells to recall responses. J Exp Med 2005; 202:123–33.
34. Zhou J, Dudley ME, Rosenberg SA, Robbins PF. Selective growth, in vitro and in vivo, of individual T cell clones from tumor-infiltrating lymphocytes obtained from patients with melanoma. J Immunol 2004;173:7622–9.
35. Yannelli JR, Hyatt C, McConnell S, Hines K, Jacknin L, Parker L, et al. Growth of tumor-infiltrating lymphocytes from human solid cancers: summary of a 5-year experience. Int J Cancer 1996;65:413–21.
36. Noonan KA, Huff CA, Davis J, Lemas MV, Fiorino S, Bitzan J, et al. Adoptive transfer of activated marrow-infiltrating lymphocytes induces measurable antitumor immunity in the bone marrow in multiple myeloma. Sci Transl Med 2015;7:288ra78.
37. Noonan K, Matsui W, Serafini P, Carbley R, Tan G, Khalili J, et al. Activated marrow-infiltrating lymphocytes effectively target plasma cells and their clonogenic precursors. Cancer Res 2005;65:2026–34.
38. Topalian SL, Drake CG, Pardoll DM. Immune checkpoint blockade: a common denominator approach to cancer therapy. Cancer Cell 2015; 27:450–61.
39. Brahmer JR, Tykodi SS, Chow LQ, Hwu WJ, Topalian SL, Hwu P, et al. Safety and activity of anti-PD-L1 antibody in patients with advanced cancer. N Engl J Med 2012;366:2455–65.
40. Rizvi NA, Mazieres J, Planchard D, Stinchcombe TE, Dy GK, Antonia SJ, et al. Activity and safety of nivolumab, an anti-PD-1 immune checkpoint inhibitor, for patients with advanced, refractory squamous non-small-cell lung cancer (CheckMate 063): a phase 2, single-arm trial. Lancet Oncol 2015;16:257–65.